6ICEGE 6th International Conference on Earthquake Geotechnical Engineering
1-4 November 2015
Christchurch, New Zealand

Effects of Non-Synchronous Ground Motion Induced by Site Conditions on the Seismic Response of Multi-Span Viaducts

M. C. Capatti[1], S. Carbonari[2], F. Dezi[3], G. Leoni[4], M. Morici[5], F. Silvestri[6], G. Tropeano[7]

ABSTRACT

The paper focuses on the effects of the spatial variability of ground motion induced by local site conditions on the seismic response of multi-span viaducts on pile foundations. Analyses are performed accounting for the soil-structure interaction: the kinematic interaction problem is formulated in the frequency domain and lumped parameter models are adopted to reproduce the frequency-dependent behaviour of the soil-foundation system in the non-linear inertial interaction analysis. Effects of the non-synchronous seismic action on the seismic response of a long bridge founded on a soft soil deposit overlying an inclined bedrock are investigated. Comparisons with results achieved with synchronous seismic motions demonstrate the significance of site effects on the response of long bridges.

Introduction

Evidences have demonstrated that, especially for long bridges, the spatial variability of ground motion may be responsible for not negligible additional forces and deformations in structural members (e.g. Monti et al., 1996; Lupoi et. 2005); moreover, SSI may sensibly affect the superstructure response, being impossible to a priori establish whether the effects are beneficial or detrimental with respect to the individual structural components (Carbonari et al., 2011).

The spatial variability of ground motion (often referred to as "*non synchronism*" of ground motion) can be attributed to three main factors: (*i*) the different arrival times of seismic waves at each site due to the finite propagation velocity (*wave-passage effect*); (*ii*) the loss of coherency induced by multiple refractions, reflections and interferences of the incident seismic waves and (*iii*) the different local soil conditions at each support of the bridge (Zerva and Zervas, 2002). The latter may be responsible of significant variation of the ground motion amplitude and frequency content between different supports. Moreover, because of the kinematic interaction, the motion experienced by the foundation differs from the free-field motion by additional translational and rotational components.

[1]Ms, DICEA, Università Politecnica delle Marche, Ancona, Italy, m.c.capatti@univpm.it
[2]Assistant Professor, DICEA, Università Politecnica delle Marche, Ancona, Italy, s.carbonari@univpm.it
[3]Assistant Professor, DESD, University of San Marino, San Marino, San Marino, francesca.dezi@unirsm.it
[4]Full Professor, SAD, University of Camerino, Camerino, Italy, graziano.leoni@unicam.it
[5]Ph.D, DICEA, Università Politecnica delle Marche, Ancona, Italy, m.morici@univpm.it
[6]Full Professor, DICEA, Federico II University, Naples, Italy, francesco.silvestri@unina.it
[7]Assistant Professor, DICAAR, University of Cagliari, Cagliari, Italy, giuseppe.tropeano@unica.it

With reference to bridges, there is a fair number of works in the literature dealing with spatial variability of ground motion in which the above factors are often studied separately to capture the relevant contributions to the structural response (e.g. Abrahamson et al., 1991; Monti et al., 1996). However, only few works include SSI analysis (e.g. Sextos et al., 2003).

In this paper, the effects of the non-synchronous ground motion, induced by site amplification, on the seismic response of multi-span viaducts on pile foundations are investigated by means of a numerical methodology that allows for including the SSI analysis. Following the substructure approach, the kinematic interaction analysis of the soil-foundation system is formulated in the frequency domain by adopting the model of Dezi et al. (2009), while the inertial interaction analysis is carried out in the time domain to account for the non-linear structural behaviour. The frequency-dependent behaviour of the soil-foundation system is included through the Lumped Parameter Model (LPM) (Wolf, 1994). The methodology is adopted to predict the seismic response of a multi-span bridge founded on a soft soil deposit characterized by an inclined soil-bedrock interface. The reference input motion is defined by a set of real accelerograms and 1D site response analyses are performed to simulate stratigraphic amplification at each support. The bridge response is compared with that obtained considering a horizontal bedrock.

Analysis Methodology

A generic bridge founded on N pile groups is considered (Figure 1*a*). Assuming that the non-linear behaviour of the soil-foundation system may be studied through a linear equivalent approach, the SSI problem can be handled according to the substructure method, addressing the kinematic problem in the frequency domain. By neglecting the interaction between pile groups supporting different piers, the soil-foundation system relevant to each pier is studied separately, making use of the finite element model proposed by Dezi et al. (2009) for the kinematic interaction analysis of pile groups. For the i-th foundation, the following system of complex linear equations, governing the dynamic problem, may be assembled:

$$\left[\begin{array}{c|c} \mathbf{Z}_{CC} & \mathbf{Z}_{CE} \\ \hline \mathbf{Z}_{EC} & \mathbf{Z}_{EE} \end{array}\right]_{F,i} \left[\begin{array}{c} \mathbf{d}_{C} \\ \hline \mathbf{d}_{E} \end{array}\right]_{i} = \left[\begin{array}{c} \mathbf{f}_{C} \\ \hline \mathbf{f}_{E} \end{array}\right]_{i} \tag{1}$$

where $\mathbf{Z}$ is the dynamic stiffness matrix of the system, $\mathbf{f}$ is the vector of nodal forces and $\mathbf{d}$ is the vector of nodal displacements, which are suitably partitioned in order to highlight components of the embedded piles (E) and of the rigid cap (C) (Figure 1*b*). According to the adopted model, matrix $\mathbf{Z}$ accounts for soil-pile and pile-soil-pile interaction, while $\mathbf{f}$ collects the soil-pile interaction forces arising as a consequence of the seismic soil motion; they are defined as:

$$\left[\begin{array}{c|c} \mathbf{Z}_{CC} & \mathbf{Z}_{CE} \\ \hline \mathbf{Z}_{EC} & \mathbf{Z}_{EE} \end{array}\right]_{F,i} = \mathbf{A}_i^T \left(\mathbf{K}_{P,i} - \omega^2 \mathbf{M}_{P,i} + \mathbf{Z}_{P,i}\right)\mathbf{A}_i \qquad \left[\begin{array}{c} \mathbf{f}_{C} \\ \mathbf{f}_{E} \end{array}\right]_{i} = \mathbf{A}_i^T \mathbf{Z}_{P,i} \mathbf{d}_{ff,i} \tag{2a, b}$$

In Equation (2), $\boldsymbol{A}_i$ is a geometric matrix enforcing the kinematic constraint at the head of the i-th pile group**,** while $\mathbf{K}_{P,i}$ and $\mathbf{M}_{P,i}$ are the frequency-independent stiffness and mass matrices of piles, respectively, $\mathbf{Z}_{P,i}$ is the complex frequency-dependent impedance matrix of the unbounded soil and $\mathbf{d}_{ff,i}$ is the free-field displacement vector within the deposit at the location of the i-th

foundation.

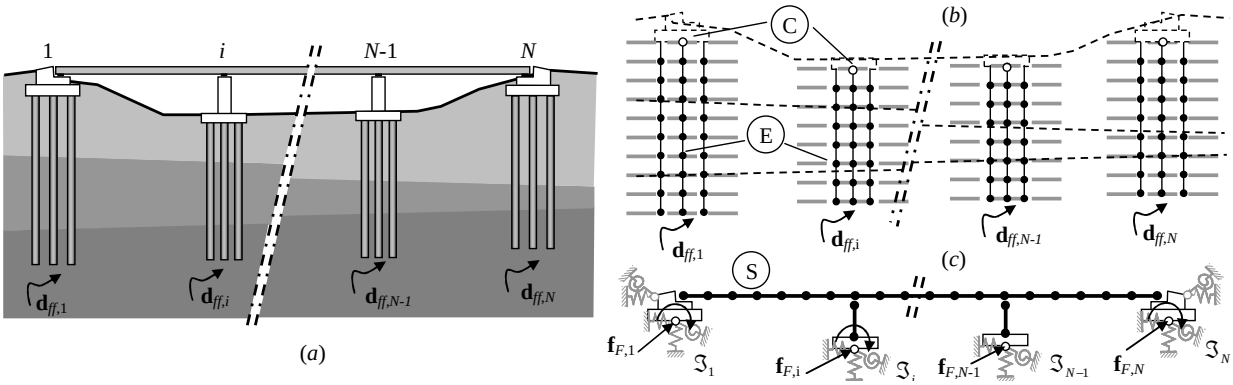

Figure 1. (*a*) Whole system; (*b*) model for soil-foundation system, (*c*) superstructure system

Being the free-field displacement vector potentially different at each foundation, the approach allows for including non-synchronism effects induced by the local soil conditions; these may be captured by performing either independent 1D S-wave propagation analyses under each support or an unique 2D or 3D seismic response analysis. By simply manipulating system (1), the soil-foundation impedance matrix $\Im_i$ and the foundation input motion, $\mathbf{d}_C$, necessary to perform inertial soil-structure interaction analysis, may be derived as follows:

$$\Im_i = \mathbf{Z}_{CC,F,i} - \mathbf{Z}_{CE,F,i}\mathbf{Z}_{EE,F,i}^{-1}\mathbf{Z}_{EC,F,i} \qquad \mathbf{d}_{C,i} = \Im_i^{-1}\left(\mathbf{f}_{C,i} - \mathbf{Z}_{CE,F,i}\mathbf{Z}_{EE,F,i}^{-1}\mathbf{f}_{C,i}\right) \qquad (3a, b)$$

The inertial interaction analysis is performed in the time domain to reproduce the non-linear behaviour of the superstructure. The frequency-dependent dynamic behaviour of the soil-foundation system is simulated by introducing suitable LPMs with frequency-independent parameters at the base of the superstructure (Wolf, 1994). Impedances of LPMs $\tilde{\Im}_i$ must approximate those of the soil-foundation system $\Im_i$ within the frequency range in which the input motion has the highest energy content and within which the fundamental periods of the structural vibration modes fall; the range 0÷10 Hz is usually considered for this purpose. From above, the dynamic stiffness matrix may be re-formulated for the *i*-th pile group as follows:

$$\left[\begin{array}{c|c}\mathbf{Z}_{CC} & \mathbf{Z}_{CE} \\ \hline \mathbf{Z}_{EC} & \mathbf{Z}_{EE}\end{array}\right]_{F,i} \cong \left[\begin{array}{c|c}\mathbf{K}_{CC} & \mathbf{K}_{CH} \\ \hline \mathbf{K}_{HC} & \mathbf{K}_{HH}\end{array}\right]_{LPM,i} - \omega^2\left[\begin{array}{c|c}\mathbf{M}_{CC} & \mathbf{0} \\ \hline \mathbf{0} & \mathbf{M}_{HH}\end{array}\right]_{LPM,i} + i\omega\left[\begin{array}{c|c}\mathbf{C}_{CC} & \mathbf{C}_{CH} \\ \hline \mathbf{C}_{HC} & \mathbf{C}_{HH}\end{array}\right]_{LPM,i} \qquad (4)$$

where subscript *H* refers to internal degrees of freedom of the LPM. **K**, **M** and **C** are positive definite stiffness, mass and damping matrices, respectively, with frequency-independent components. The foundation input motion (FIM) is applied at the base of the superstructure by considering forces acting at the caps of pile groups; for the *i*-th group, these forces are transformed in the time domain with the following expression:

$$\mathbf{f}_{F,i}(t) = \frac{1}{2\pi}\int_{-\infty}^{\infty}\tilde{\Im}_i\mathbf{d}_{FIM,i}e^{j\omega t}d\omega \qquad (5)$$

The inertial interaction problem of the discrete system (Figure 1*c*) may be formulated as:

$$\begin{bmatrix} \mathbf{M}_{SS} & \mathbf{0} \\ \mathbf{0} & \mathbf{M}_{FF}+\mathbf{M}_{LPM} \end{bmatrix} \begin{bmatrix} \ddot{\mathbf{u}}_S \\ \ddot{\mathbf{u}}_F \end{bmatrix} + \begin{bmatrix} \mathbf{C}_{SS} & \mathbf{C}_{SF} \\ \mathbf{C}_{FS} & \mathbf{C}_{FF}+\mathbf{C}_{LPM} \end{bmatrix} \begin{bmatrix} \dot{\mathbf{u}}_S \\ \dot{\mathbf{u}}_F \end{bmatrix} + \begin{bmatrix} \mathbf{0} & \mathbf{0} \\ \mathbf{0} & \mathbf{K}_{LPM} \end{bmatrix} \begin{bmatrix} \mathbf{u}_S \\ \mathbf{u}_F \end{bmatrix} + \mathbf{f}_{NL}(\mathbf{u},\dot{\mathbf{u}}) = \begin{bmatrix} \mathbf{0} \\ \mathbf{f}_F \end{bmatrix} \quad (6)$$

where $\mathbf{M}$ is the mass matrix of the system, obtained by assembling structural masses ($\mathbf{M}_{SS}$ and $\mathbf{M}_{FF}$ relevant to masses of the deck, piers and foundation caps) and masses of LPMs ($\mathbf{M}_{LPM}$), $\mathbf{C}$ is the damping matrix resulting from the relevant contributions of LPMs ($\mathbf{C}_{LPM}$) and of the structure. The latter may be calibrated on the basis of the tangent stiffness matrix, in order to assure a target structural damping (usually 5%). Furthermore, $\mathbf{K}_{LPM}$ is the stiffness matrix obtained by considering contributions of LMPs and $\mathbf{f}_{NL}$ is the vector of the non-linear restoring forces of the system. Finally, $\mathbf{f}_F$ is the vector collecting forces evaluated with Equation (5) by considering the different foundation input motions at each pier.

Case Study

The previous procedure is adopted to investigate effects of spatial variation of ground motion induced by site effects on the seismic response of a long multi-span viaduct, taking SSI into account. In particular, the 10-span viaduct with continuous steel-concrete composite deck reported in Figure 2*a*, *b* is considered. The bridge is one of those already considered by Carbonari et al. (2012) for studying soil-structure interaction effects in the case of uniform soil conditions. Under dynamic loading, the bridge is fixed at all piers (P#) while multi-directional bearings are used in order to avoid a double-path resisting mechanism that would strongly drive the deck. Foundations are constituted by groups of bored r.c. piles with diameter d = 1.2 m, length L_p = 30 m and spacing $s = 3d$ (Figure 2*c*). For the present application, a soft soil deposit overlying a seismic bedrock is considered; the interface plane, parallel to the transverse direction of the bridge, is either horizontal (HB configuration) or sloped 15° (IB configuration), so that the bedrock depth at the middle bridge support is equal to 97 m, for both cases (Figure 2*a*). The deposit is constituted by normally consolidated clays with properties reported in Figure 2*d*; the variability with depth of the small strain shear modulus (G_0) is defined according to empirical formulas (d'Onofrio and Silvestri, 2001). The resulting shear wave velocity profile (Figure 2*e*) corresponds to an equivalent $V_{s,30}$ (149 m/s) falling in the range defined by EN1998-1 for soil class D. The bedrock has shear wave velocity $V_{s,b}$ = 1000 m/s and density ρ_b = 2.0 Mg/m^3. The seismic design of the bridge is simulated according to a direct displacement-based approach, by considering a single pier clamped at the base. The type I elastic displacement response spectrum defined by EN1998-1 for soil class D is adopted with an amplified Peak Ground Acceleration (PGA) of 0.47g, corresponding to a reference 0.35g in soil type A. The 15 m high circular piers of diameter D = 2.4 m are designed to withstand the displacement demand with an expected ductility $\mu \approx 2$. Further details of the bridge design can be found in Carbonari et al. (2012).

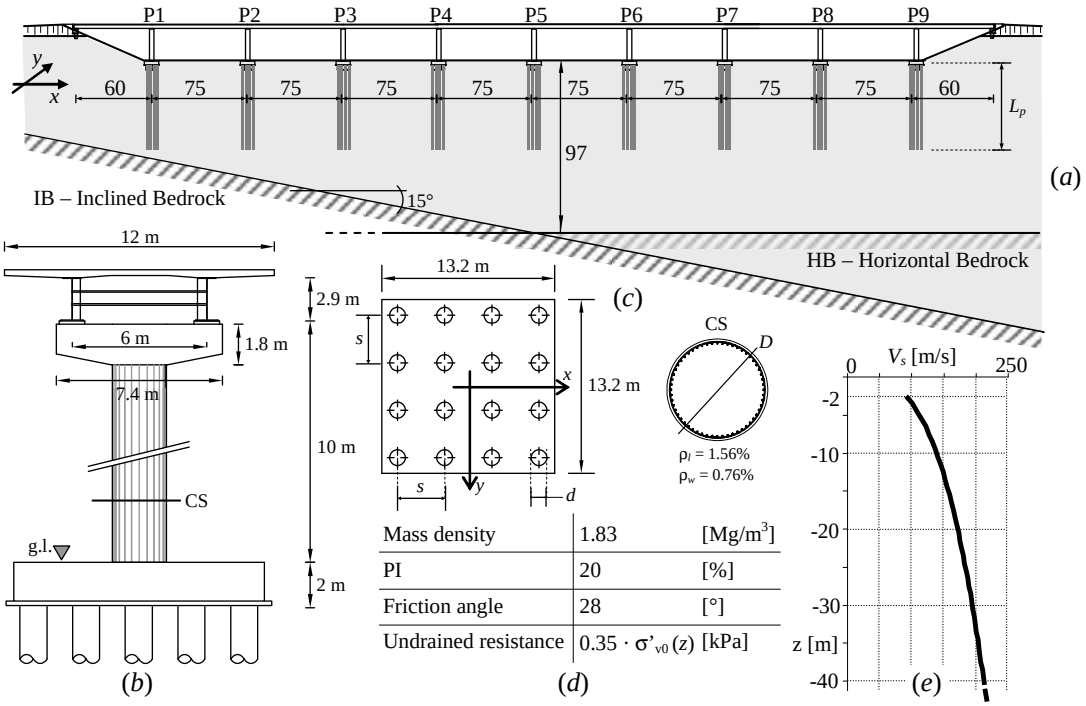

Figure 2. (*a*) Lateral view of the viaduct; (*b*) pier elevation; (*c*) foundation and pier cross section; (*d*) soil mechanical properties and (*e*) V_s profile down to 40 m

Non Synchronous Seismic Input due to Site Effects

The reference input motion is constituted by a set of seven real records defined at outcropping bedrock and selected so that their mean acceleration elastic response spectrum, normalised with respect to PGA, matches the relevant spectrum suggested by EN1998-1 for soil type A. The input motions, reported in Table 1, are characterized by 2 orthogonal horizontal components digitized by free-field stations located on rock outcrop, with magnitude, M_w, ranging between 5 and 7, and epicentral distances, Δ, less than 30 km. The signals are scaled in order to obtain the design hazard level; the mean scale factor (S.F.) adopted is about 4.3. Figure 3*a* shows the mean elastic acceleration response spectra of longitudinal (*x*) and transverse (*y*) components of the selected records, compared with the code reference spectrum. Spectra relevant to all records are reported with light grey lines to provide a pictorial view of the input variability.

Independent 1D site response analyses are performed in the *x* and *y* directions to capture stratigraphic amplification effects and to evaluate the non-synchronous seismic motion at the ground surface. A linear equivalent model is used for the soil, updating shear modulus and damping consistently with the maximum strain level attained during the shaking on the basis of the standard curves suggested by Vucetic and Dobry (1991) for clays of comparable plasticity. Due to the high motion amplitude and soil deformability, the maximum shear strain often resulted higher than the volumetric threshold strain equal to 0.05%, indicated by Vucetic (1994) for a typical clay with PI=20%; also, the peak shear stress was sometimes checked to trespass the undrained strength. Nevertheless, soil shear-volumetric coupling and local failure, which are expected to induce energy dissipation and therefore a reduction of the seismic actions transmitted to the piers, were conservatively neglected in these pilot analyses. Figures 3*b* and *c* show the

mean elastic response spectra obtained at the ground surface at the location of each pier, compared with the code-specified spectrum for soil type D.

Table 1. Selected earthquake

Earthquake	Station	Date	M_w	Δ [km]	PGA [g] (*x*/*y*)	S.F. (*x*/*y*)
Campano Lucano	Auletta	23/11/80	6.9	25	0.06 / 0.06	5.84/5.84
Lazio Abruzzo	Ponte Corvo	07/05/84	5.9	22	0.06 / 0.07	5.47/5.12
Umbria Marche (aftershock)	Cascia	14/10/97	5.6	23	0.05 / 0.06	6.55/8.89
South Iceland (aftershock)	Flagbjarnarholt	21/06/00	6.4	22	0.05 / 0.04	6.69/8.89
South Iceland (aftershock)	Selfoss-CH	21/06/00	6.4	15	0.13 / 0.12	2.75/3.03
South Iceland	Flagbjarnarholt	17/06/00	6.5	21	0.32 / 0.34	1.10/1.04
Montenegro	Ulcinnj	15/04/79	6.9	21	0.18 / 0.22	1.93/1.56

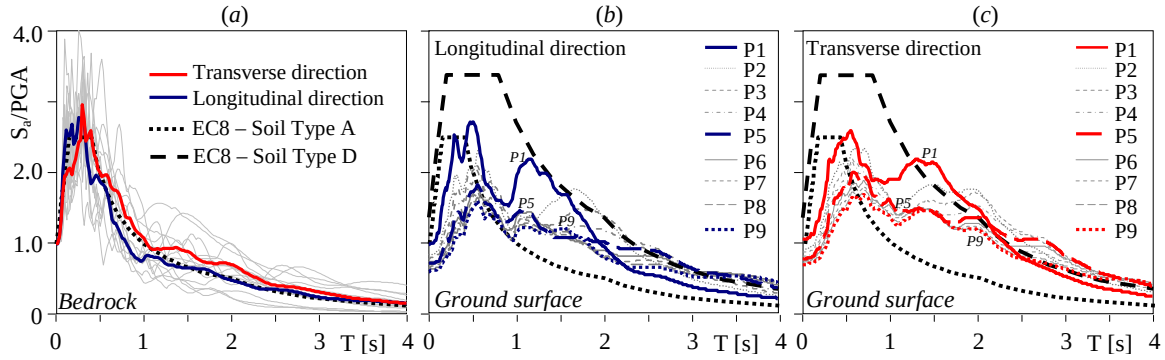

Figure 3. Mean acceleration response spectra of the selected input motions (*a*) and at ground surface of each support along longitudinal (*b*) and transverse (*c*) directions

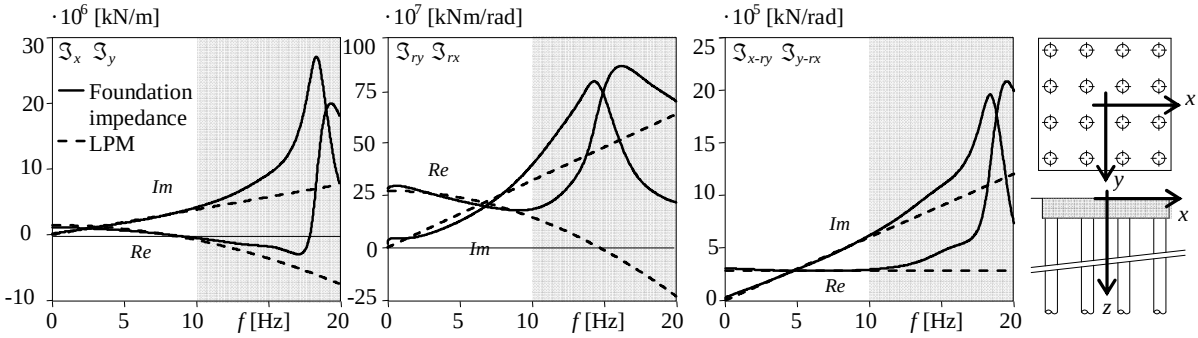

Figure 4. Components of the soil-foundation system impedance matrix

Spectral amplifications are evident at all piers for periods greater than 1 s, and result overall consistent with those quantified by the code; moving from P1 to P9, the period corresponding to the highest amplification increases, as a consequence of the increasing bedrock depth. It is worth noting that results obtained for P5 are representative of the HB configuration of the soil deposit.

Kinematic and Inertial Interaction Analyses

Analyses of the soil-foundation systems are performed with the numerical model proposed by Dezi et al. (2009); the piles, modelled with 1 m long beam elements, have density $\rho_p = 2.5$ Mg/m³ and Young's modulus $E_p \approx 23.5$ GPa to account for concrete cracking. Figure 4 shows the translational, rotational and coupled roto-translational components of the impedance matrix for the piers foundation (solid lines). For the sake of simplicity, the small-strain shear modulus is adopted to evaluate the soil-pile impedance so that, according to Dezi et al. (2009), the dynamic stiffness of the soil-foundation system is the same at all the bridge supports.

Non-linear analyses of inertial interaction are carried out in time domain, developing a 3D finite element model of the bridge. Linear elastic beam elements are used for the deck, while fiber elements are adopted for piers to capture their non-linear behaviour under bidirectional excitation. Cross-section properties of members are based on the suggestions by Mander et al. (1988) for confined and unconfined concrete and by Menegotto and Pinto (1973) for rebars. Furthermore, 5% structural damping is introduced in terms of tangent stiffness proportional damping. Figure 4 shows the impedances of the LPMs (Carbonari et al., 2012), calibrated to approximate the behaviour of the soil-foundation system in the range 0÷10 Hz (dashed lines).

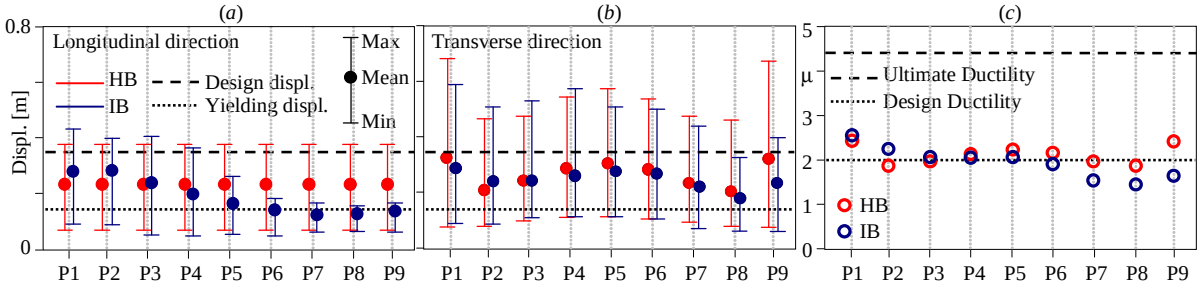

Figure 5. Deck displacements in (*a*) longitudinal (*b*) transverse direction; (*c*) ductility demand

The foundation input motion is represented by generalised forces applied at the level of pile caps. For IB configuration, the seismic actions are different at each pier and account for the site-induced non-synchronism. Conversely, the FIM relevant to HB configuration is synchronous at all supports and is the same as that obtained for pier P5.

Main Results

The effects of the spatial variability of ground motion due to site effects on the non-linear seismic response of the case study can be assessed comparing the results obtained for IB and HB configurations. For the sake of brevity, only few results will be shown in terms of mean values obtained from the non-linear dynamic analyses performed with the whole set of accelerograms.

Figure 5*a* and *b* shows the peak values of the relative displacements of the deck with respect to the foundation, in the longitudinal and transverse directions, respectively. The spatial variability of ground motion (IB configuration) affects sensibly displacements in the longitudinal direction as a consequence of the coupling effect exerted by the rigid deck which enforces the piers top to undergo the same movements in the *x* direction. In this direction displacements at P6-P7-P8-P9

are about one half those obtained for HB configuration. In the transverse direction very slight differences can be observed between displacements resulting from HB and IB configurations.

Figure 5*c* compares the displacement ductility demand of each pier, evaluated with reference to the combined longitudinal and transverse displacements resulting from HB and IB configurations, by suitably accounting for the effects of the foundation rigid rotation. The ductility demand is almost coincident with the design one (dotted line) and is far from the ultimate ductility (dashed line). Effects of the spatial variability of ground motion are evident at the edge piers and particularly at piers with thicker soil deposits (P7-P8-P9) where a significant decrease of the ductility demand is observed, consistently with the reduction of the longitudinal and transverse displacements.

Conclusions

A numerical methodology to include effects of non-synchronous seismic motion induced by local stratigraphic conditions in the SSI analysis of multi-span viaducts on pile foundations has been presented. The kinematic interaction analysis is formulated in the frequency domain, while the inertial interaction analysis is carried out in the time domain, to include the non-linear structural behaviour. The methodology is applied to a case study constituted by a multi-span bridge founded on a soft soil deposit overlying an inclined bedrock. The reference input motions is represented by a set of suitably selected real accelerograms, and the spatial variability of ground motion due to site effects is evaluated with 1D site response analyses. The structural response obtained by considering the spatial variation of ground motion is compared with that resulting from the application of a synchronous action. The specific soil conditions at each bridge support play a key role in the definition of the seismic action. The application demonstrates that the spatial variability of the seismic motion due to site effects is crucial for a reliable prediction of the structural response. Even if only effects on deck displacements and ductility demand of piers have been shown for the sake of brevity, local effects on the deck bearing supports are also expected to be important. Future developments will focus on the role of soil non-linearity and plastic straining by means of 1D non-linear analyses and on the role of the buried bedrock geometry by means of 2D seismic response analyses.

References

Abrahamson NA, Schneider JF, Stepp JC. Empirical spatial coherency functions for application to soil-structure to soil-structure interaction analyses. *Earthq. Spectra*, 1991; **7**(2): 1-27.

Carbonari S, Dezi F, Leoni G. Seismic soil-structure interaction in multi-span bridges: application to a railway bridge. *Earthq. Eng. & Struct. Dyn.*, 2011; **40** (11): 1219-1239.

Carbonari S, Morici M, Dezi F, Nuti C, Silvestri F, Tropeano G., Vanzi I. Seismic response of viaducts accounting for soil-structure interaction. *15 WCEE 2012*, Lisbon, Portugal, Sept. 2012, paper n.4150.

Dezi, F, Carbonari S, Leoni G. A model for the 3D kinematic interaction analysis of pile groups in layered soils. *Earthquake Engng Struct. Dyn*., 2009; **38** (11): 1281–1305.

Dezi F, Carbonari S, Tombari A, Leoni G. Soil-structure interaction in the seismic response of an isolated three-span motorway overcrossing founded on piles. *Soil Dyn. & Earthq. Eng*., 2012; **41**: 151-163.

d'Onofrio A, Silvestri F. Influence of micro-structure on small-strain stiffness and damping of fine grained soils and effects on local site response. IV Int. Conf. on *'Recent Advances in Geotech. Earthquake Engng and Soil Dynamics'*, 2001, S. Diego, CA. Paper 1.19.

EN 1998-1, 2004 *Eurocode 8: Design of structures for earthquake resistance - Part 1: General rules, seismic actions and rules for buildings.*

Lupoi A, Franchin P, Monti G, Pinto PE. Seismic design of bridges accounting for spatial variability of ground motion. *Earthq. Eng. & Struct. Dyn*., 2005; **34**: 327-348.

Mander JB, Priestley MJN, Park R. Theoretical stress-strain model for confined concrete. *Journal of Structural Engineering*, ASCE, 1988: **114** (8): 1804-826.

Menegotto M, Pinto PE. Method of analysis for cyclically loaded R.C. plane frames including changes in geometry and non-elastic behaviour of elements under combined normal force and bending. *Symp. on the resistance and ultimate deformability of structures acted on by well defined repeated loads*, Zurich, Switzerland, 1973, 15-22.

Monti G, Nuti C, Pinto PE. Nonlinear response of bridges under multisupport excitation. *ASCE Jnl Struct. Eng*. 1996; **122** (10):1147-1159.

Sextos AG, Pitilakis KD, Kappos AJ. Inelastic dynamic analysis of RC bridges accounting for spatial variability of ground motion, site effects and soil-structure interaction phenomena. Part 2: Parametric study. Earthquake Engng *Struct. Dyn*., 2003; **32** (4): 629-52.

Vucetic M, Dobry R. Effect of soil plasticity on cyclic response. *Journ. of Geot. Eng.* ASCE, 1991; **117** (1), 89-107.

Vucetic M. Cyclic threshold shear strains in soils. *Journ. of Geot. Eng.* ASCE, 1994, **120** (12), 2208-2228.

Wolf JP. *Foundation vibration analysis using simple physical models*, Prentice-Hall: Englewood Cliffs N.J., 1994.

Zerva A, Zervas V. Spatial variation of seismic ground motions: an overview. *Appl. Mech. Rev*. 2002: **55** (3): 271-297.